

FULL PAPER

Open Access



# Mass-related excitation of polar motion: an assessment of the new RL06 GRACE gravity field models

Franziska Göttl<sup>\*</sup> , Michael Schmidt and Florian Seitz

## Abstract

The new Release-06 (RL06) Gravity Recovery and Climate Experiment (GRACE) gravity field solutions are evaluated by converting them into equatorial effective angular momentum functions (so-called excitation functions) for polar motion and comparing these to respective time series based on space-geodetic observations (geodetic excitation). The same is performed for the older RL05 solutions using identical processing. Maps of equivalent water heights derived from both releases show that the signal-to-noise ratio is significantly improved in RL06. The derived polar motion excitation functions from RL05 and RL06 differ by about 15%. An analysis of the contributions of different Earth subsystems revealed that the release update mainly influenced the hydrological (12%) and oceanic excitations (17%), but it has a relatively small impact on the cryospheric excitations related to Antarctica (4%) and Greenland (1%). The RL06 data from different GRACE processing centers are more consistent among each other than the previous RL05 data. Comparisons of the GRACE-based excitation functions with the geodetic and model-based oceanic excitations show that the latest release update improved the agreement by about 2 to 15 percentage points.

**Keywords:** GRACE RL06 gravity field models, Polar motion excitation, Effective angular momentum functions

## Introduction

Mass displacements within the Earth system cause variations of the Earth's gravity field and its rotation. Thus, temporal variations of the gravity field can be used to study the mass-related excitation of polar motion. By separating the observed integral gravity signal into contributions from different Earth subsystems, also individual mechanisms of polar motion excitation can be studied. Most important are the variations of the degree-2 spherical harmonic potential coefficients  $C_{21}$  and  $S_{21}$  as these are directly related to polar motion excitation (Barnes et al. 1983).

Between 2002 and 2017, the satellite gravity mission Gravity Recovery and Climate Experiment (GRACE) observed the time variable gravity field of the Earth. The GRACE science teams at the Center for Space Research (CSR), Austin, the GeoForschungsZentrum (GFZ),

Potsdam, and the Jet Propulsion Laboratory (JPL), Pasadena, provide monthly GRACE gravity field solutions. In irregular time intervals release updates were performed: 2003 (RL01), 2005 (RL02 and RL03), 2007 (RL04), 2012 (RL05) and recently in 2018 (RL06). A lot of studies exist in which GRACE RL05 gravity field solutions have been used to estimate the integral as well as individual mass-related effects on Earth rotation (e.g., Adhikari and Ivins 2016; Chen et al. 2013, 2017; Göttl et al. 2015; Malgorzata et al. 2017; Meyrath and van Dam 2016). It was shown that due to the release update from RL04 to RL05 the agreement between GRACE-derived effective angular momentum functions and the mass-related part of the so-called geodetic excitations (Brzeziński 1992) could be slightly improved. The latter can be derived from Earth Orientation Parameter (EOP) time series, such as EOP 14 C04 (Bizouard et al. 2014) of the International Earth Rotation and Reference Systems Service (IERS), reduced by the motion-related effects within the atmosphere (winds) and oceans (currents) based on geophysical model data. Recently, CSR, JPL and GFZ have produced

\*Correspondence: franziska.goettl@tum.de  
Deutsches Geodätisches Forschungsinstitut, Technische Universität München, Arcisstraße 21, 80333 Munich, Germany

**Table 1 Background models used within the RL05 and RL06 GRACE gravity field processing**

Gravity field model	Mean gravity	Solid Earth tides	Ocean tides	Pole tide	Short-term variations	N body perturbations
CSR RL05	GIF48	IERS 2010	GOT4.8	IERS 2010 (cubic)	AOD1B RL05	DE 405
JPL RL05	GIF48	IERS 2010	GOT4.7	IERS 2010 (cubic)	AOD1B RL05	DE 421
GFZ RL05	EIGEN-6C	IERS 2010	EOT11a	Constant mean pole	AOD1B RL05	DE 421
ITSG-Grace2016	GOCO04s	IERS 2010	EOT11a	IERS 2010 (cubic)	AOD1B RL05	DE 421
CSR RL06	GGM05C	IERS 2010	GOT4.8	IERS 2010 (linear)	AOD1B RL06	DE 430
JPL RL06	GGM05C	IERS 2010	FES2014b	IERS 2010 (linear)	AOD1B RL06	DE 430
GFZ RL06	EIGEN-6C4	IERS 2010	FES2014	IERS 2010 (linear)	AOD1B RL06	DE 430
ITSG-Grace2018	ITSG-GraceGoce2017	IERS 2010	FES2014b + GRACE	IERS 2010 (linear)	AOD1B RL06 + LSDM	DE 421

the new RL06 GRACE gravity field solutions applying improved parameters, processing algorithms, data editing and background gravity models. Accordingly, the Institute of Theoretical Geodesy and Satellite Geodesy (ITSG) of the Graz University of Technology provides the new ITSG-Grace2018 monthly and daily gravity field models which also incorporate the new RL06 background gravity models. In particular, the degree-2 potential coefficients  $C_{21}$  and  $S_{21}$  are influenced by the change of the mean pole model from cubic to linear. The goal of this study is to analyze the new RL06 GRACE data regarding its consistency with the mass-related part of the geodetic excitation of polar motion (integrally and for individual subsystems), to quantify the improvement of RL06 data with respect to RL05, and to study the differences of the solutions from CSR, JPL, GFZ and ITSG.

The paper is outlined as follows: the next section provides an overview of the GRACE gravity field models [RL05 and RL06 from CSR, JPL and GFZ as well as the GRACE gravity field models ITSG-Grace2016 (incorporating the RL05 background models) and ITSG-Grace2018 (incorporating the RL06 background models)] and the processing steps in order to determine the equatorial effective angular momentum functions for polar motion excitation. Further, we introduce the time series EOP 14 C04 and the steps for the separation of the mass-related part of the geodetic excitation that will be used for the comparison with the GRACE-derived excitation in the third section. There, also maps of equivalent water heights from GRACE RL05 and RL06 data are analyzed with respect to the signal-to-noise ratio and the consistency of the solutions of the processing centers. Finally, the last section provides the conclusions.

## Data and data processing

### GRACE gravity field solutions

In this study, we use the RL05 and the new RL06 GRACE gravity field solutions from CSR, JPL and GFZ, namely CSR RL05 (Bettadpur 2012), CSR RL06 (Bettadpur 2018),

JPL RL05<sup>1</sup> (Watkins and Yuan 2014), JPL RL06 (Yuan 2018), GFZ RL05<sup>2</sup> (Dahle et al. 2012) and GFZ RL06 (Dahle et al. 2018). Further, we use the GRACE gravity field solutions from ITSG, namely ITSG-Grace2016 (Mayer-Gürr et al. 2016) and ITSG-Grace2018 (Mayer-Gürr et al. 2018). Beside changes in the processing algorithms and data editing, there are also significant changes in the background models as shown in Table 1. The GRACE gravity field solutions are provided as Level-2 products GSM<sup>3</sup>, GAC<sup>4</sup> and GAD<sup>5</sup>. Figure 1 shows the time series of the potential coefficients  $C_{21}$  and  $S_{21}$  of the CSR RL05 and RL06 GSM products. A significant modification of these coefficients was caused in particular by the change of the mean pole model from cubic to linear. The introduction of a new mean pole model was motivated by a significant mismatch between the cubic polygon fitted to a filtered time series of polar motion and the observed polar motion after 2010. Accordingly, the IERS Conventions (Petit and Luzum 2010) have been updated by a new conventional linear mean pole model based on the full extent of the IERS EOP C01 series (1900–2017). The relative standard deviations (RSD) of CSR RL05 and RL06 for  $C_{21}$  and  $S_{21}$  are up to 32%. The RL06 solution is smoother, especially for  $S_{21}$ , and changes of the trend are clearly visible. The new RL06 GRACE Atmosphere and Ocean De-Aliasing Level-1B (AOD1B) product (Dobslaw et al. 2017b) provides, compared to its predecessor in RL05 (Flechtner et al. 2015), an increased temporal and spatial resolution, a clear separation of tidal and non-tidal signals and an improvement of long-term consistency (Dobslaw et al. 2017a). The oceanic component

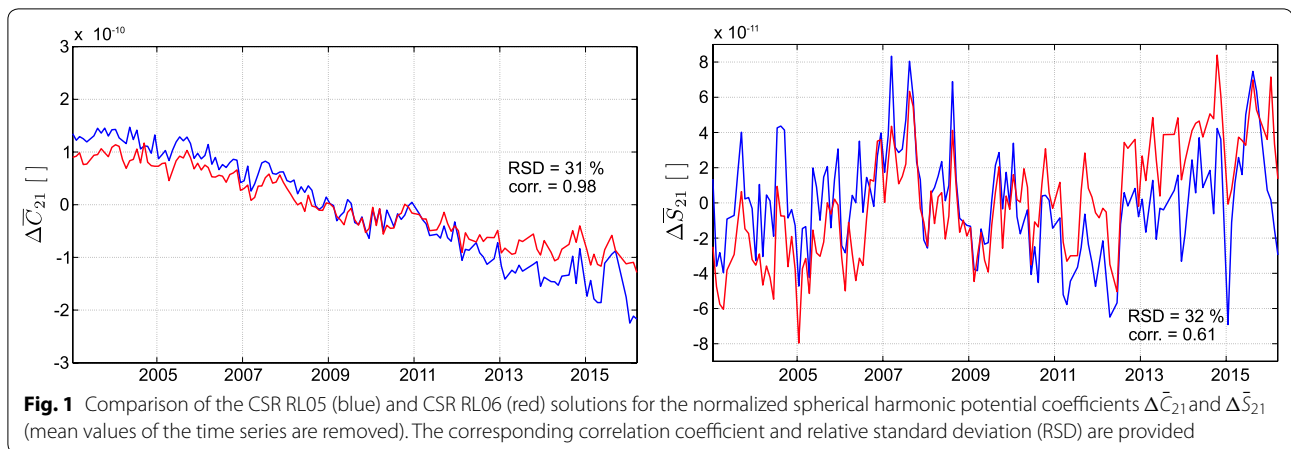
<sup>1</sup> JPL has reprocessed the RL05 dataset, the new release is officially called RL05.1; here we refer to it as RL05.

<sup>2</sup> GFZ's release is officially called RL05a; here we refer to it as RL05.

<sup>3</sup> GSM: Earth gravity field excluding tidal effects and short-term atmospheric and oceanic variations

<sup>4</sup> GAC: Non-tidal short-term effects of the atmosphere and oceans.

<sup>5</sup> GAD: Ocean bottom pressure.



is no longer based on the Ocean Model for Circulation and Tides (OMCT; Dobslaw et al. 2013) but on the Max-Planck-Institute Ocean Model (MPIOM; Jungclauss et al. 2013), while the atmospheric component is still based on atmospheric re-analysis of the European Center for Medium-Range Weather Forecasts (ECMWF). The a posteriori correction models GAE, GAF and GAG of the AOD1B RL05 product (Fagiolini et al. 2015) that account for updates at ECMWF, are no longer necessary for RL06. However, the impact of the changes in the AOD1B product on the coefficients  $C_{21}$  and  $S_{21}$  is small (14% for  $C_{21}$  and 8% for  $S_{21}$ ).

The coefficients  $C_{21}$  and  $S_{21}$  are proportional to the mass-related part of the equatorial effective angular momentum functions  $\chi_1^{\text{mass}}$  and  $\chi_2^{\text{mass}}$  that describe the excitation of polar motion (e.g., Barnes et al. 1983; Gross 2007; Wahr 2005). Conversion formulas given by Göttl (2013) are used here. While the integral excitation can be derived directly from the sum of the GSM and GAC products, individual contributions of the continental hydrosphere  $\chi^H$ , oceans  $\chi^O$ , Antarctica  $\chi^A$  and Greenland  $\chi^G$  are computed from the sum of the GSM and GAD products by applying adequate filter techniques, masks and global spherical harmonic synthesis/analysis. In this study, we use different versions of the anisotropic decorrelation filter DDK (Kusche 2007) in order to demonstrate that the signal-to-noise ratio could be significantly improved due to the release update. The degree-1 Stokes coefficients are replaced by solutions from Swenson et al. (2008) derived from GRACE data and ocean model outputs in order to account for the fact that mass displacements are referenced to a coordinate system attached to the Earth's crust which moves relative to the Earth's center-of-mass frame used in the GRACE data processing. Furthermore, as recommended, the inaccurate  $C_{20}$  coefficient of the GSM product is replaced by an improved external satellite laser ranging (SLR) solution

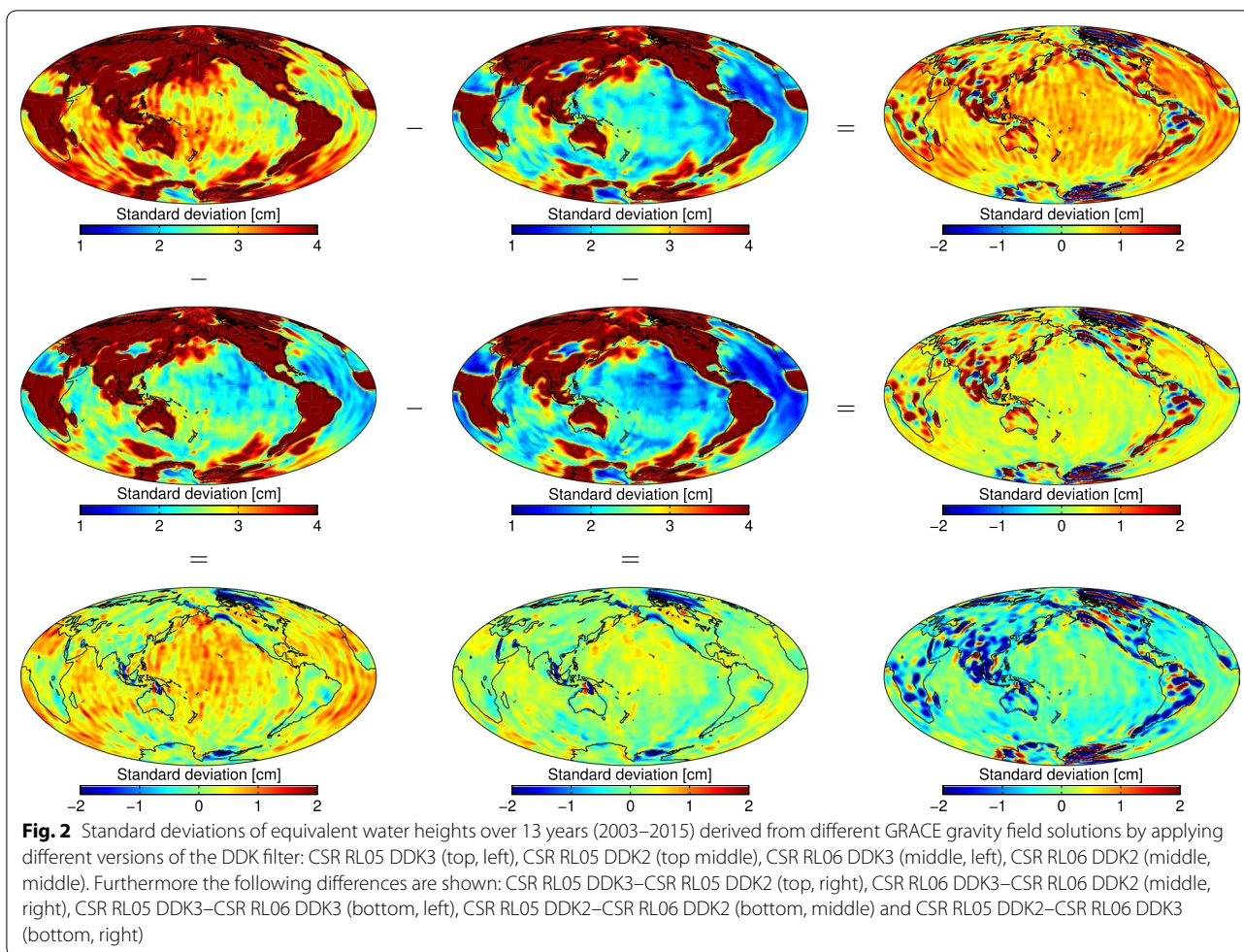
from Cheng et al. (2013) based on GRACE RL05 (GRACE Technical Note 07) or on GRACE RL06 (GRACE Technical Note 11), respectively. In order to identify individual excitations of polar motion, the effect of glacial isostatic adjustment (GIA) must be removed from the GRACE observations. We use the global GIA model IJ05\_R2 from Ivins et al. (2013).

#### Polar motion

Polar motion values are taken from the time series EOP 14 C04 of the IERS which is based on a combination of space-geodetic observation techniques (Bizouard et al. 2014). The daily pole coordinates  $x$  and  $y$  are fully consistent with the International Terrestrial Reference Frame 2014 (ITRF2014), and the mean uncertainties of the pole coordinates are below 40  $\mu\text{s}$ . From this time series, the so-called geodetic excitation of polar motion, i.e., the equatorial effective angular momentum functions  $\chi^{C04}$ , are determined by applying the conversion formulas given by Gross (1992). They represent the combined excitation from the redistribution of masses (mass effect) and their motion (motion effect) within the Earth system. In order to compare the GRACE-derived excitation with the geodetic excitation, the motion-related part needs to be reduced from the latter. This is achieved by using the geophysical model data described below.

#### Geophysical models

For the reduction of the motion-related part from the geodetic excitation, we apply geophysical model data describing the effects of wind and ocean currents as provided by the Global Geophysical Fluids Center (GGFC) of the IERS. These data are derived from two consistent atmosphere/ocean model combinations: The atmospheric re-analysis from NCEP (National Centers for Environmental Prediction; Zhou et al. 2006) in combination with the ocean model ECCO (Estimating



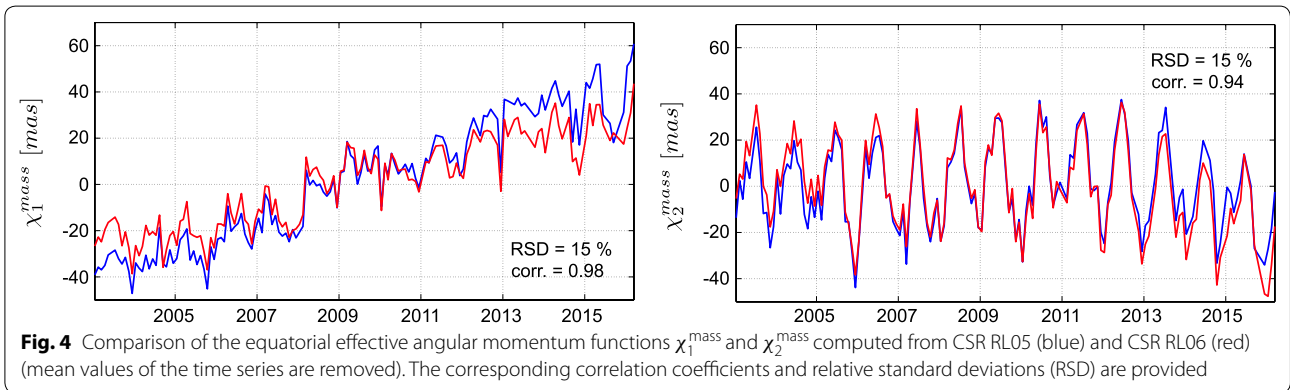
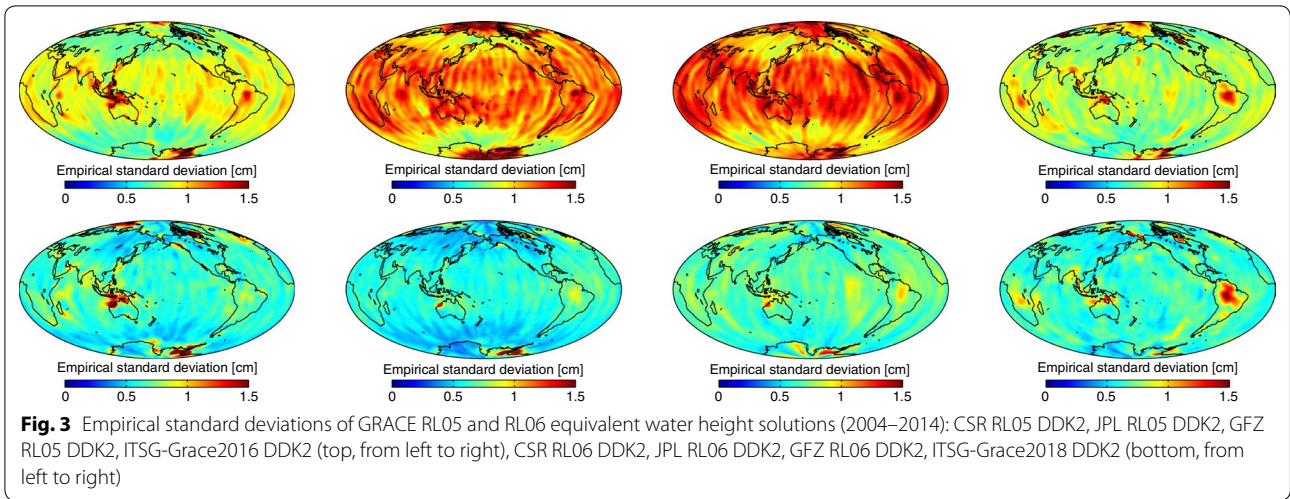
the Circulation and Climate of the Ocean; [ftp://euler.jpl.nasa.gov/sbo/oam\\_global/ECCO\\_kf079.chi](ftp://euler.jpl.nasa.gov/sbo/oam_global/ECCO_kf079.chi)) (henceforth referred to as NE), and the atmospheric and oceanic effective angular momentum functions computed by the Earth System Modelling group at Deutsches GeoForschungsZentrum (ESMGFZ) based on operational and re-analysis data from the ECMWF and the ocean model MPIOM (henceforth referred to as ESMGFZ; Dobslaw and Dill 2018). Due to the fact that the modeled motion-related effective angular momentum functions suffer from model uncertainties (in particular due to a lack of precise measurements of wind and ocean velocities on global scale), the remaining mass-related part of the geodetic excitation of polar motion  $\chi^{C04-NE}$  and  $\chi^{C04-ESMGFZ}$  is afflicted with some (unknown) uncertainty. For a comparison with the GRACE-derived oceanic excitation, we will later use the mass-related parts of the two oceanic excitation series from the ocean model ECCO and from ESMGFZ. The latter combines the effective angular momentum functions for the dynamic ocean (OAM) and for the

barystatic sea-level (SLAM) to take into account the inflow of terrestrial water into the oceans.

## Results and comparisons

### Mass redistribution within the Earth system

Mass changes within the Earth system are commonly expressed in terms of equivalent water heights (Wahr et al. 1998). Figure 2 shows the standard deviations of the GRACE-based equivalent water heights over 13 years (2003–2015) by applying the filters DDK3 ( $a = 10^{12}$ ,  $p = 4$ ) or DDK2 ( $a = 10^{13}$ ,  $p = 4$ ) in order to reduce the meridional stripes in the RL05 and RL06 GRACE gravity field solutions. The signal is significantly larger over the continents than over the oceans (the color bar of the figure is selected to visualize the differences over the oceans). One can see that the signal-to-noise ratio is significantly improved by the release update. The reduction of the meridional stripes with the DDK3 filter is much more effective for RL06 than for RL05. The signal-to-noise ratio of the solutions RL06 DDK3 lies in between the signal-to-noise ratios



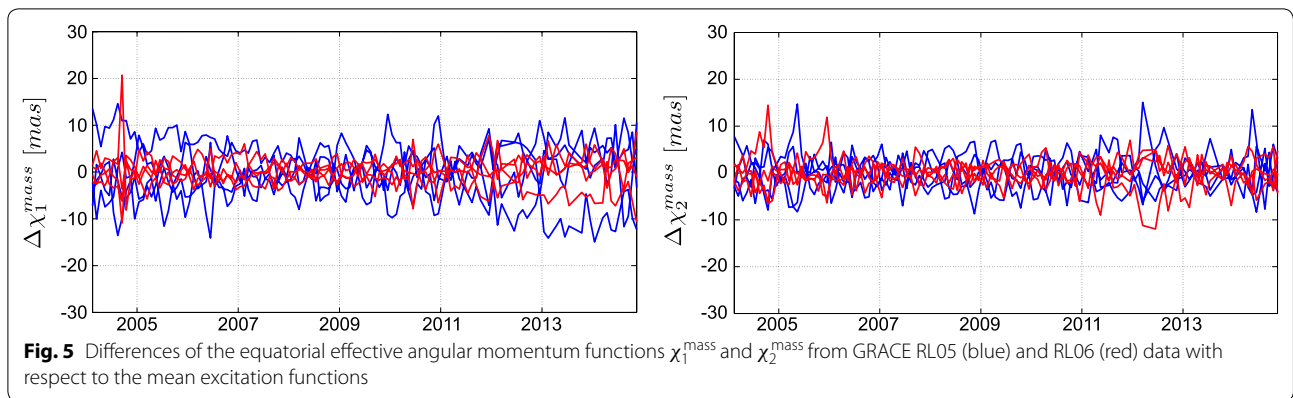
of the solutions RL05 DDK3 and RL05 DDK2. The RL06 DDK2 solutions are even smoother than the RL05 DDK2 solutions.

Figure 3 provides the empirical standard deviations of the GRACE RL05 and RL06 fields of equivalent water heights (DDK2 filter applied) from CSR, JPL, and GFZ as well as from the two ITSG solutions. Due to different processing strategies and background models (see Table 1), the equivalent water heights differ significantly in all solutions. The empirical standard deviations of the RL06 residuals are on average 0.7 cm for CSR, 0.6 cm for JPL, 0.7 cm for GFZ, and 0.7 cm for ITSG, whereas the empirical standard deviations of the RL05 residuals are on average 0.9 cm for CSR, 1.3 cm for JPL, 1.2 cm for GFZ, and 0.8 cm for ITSG. Especially in the polar regions and mid-latitudes, the differences between the solutions from CSR, JPL, GFZ and ITSG are clearly reduced by the release update. Among the RL05 models, the ITSG-Grace2016 monthly solution exhibits the smallest empirical standard deviation. For RL06, the empirical standard deviations of all investigated solutions are quite similar.

**Polar motion excitation: integral effect**

As mentioned before, equatorial effective angular momentum functions describing the integral mass-related part of the excitation functions of polar motion can directly be derived from the potential coefficients  $C_{21}$  and  $S_{21}$  (GSM + GAC). In this conversion, no filtering of the GRACE gravity field solutions is required. Figure 4 shows the equatorial effective angular momentum functions from GRACE (CSR RL05 and RL06). A difference in the trend is clearly visible for  $\chi_1^{\text{mass}}$  as well as for  $\chi_2^{\text{mass}}$ . The RSD of the polar motion excitation functions amount to 15%.

In analogy to the previous section, we also investigate the differences of the excitation functions derived from the GRACE RL06 solutions from CSR, JPL, and GFZ and ITSG-Grace2018. Like for the equivalent water heights, the differences between the excitation functions from the different GRACE solutions are much smaller for RL06 than for RL05 (see Fig. 5 and Table 2). The release update improves the agreement of the derived  $\chi_1^{\text{mass}}$  series by about 5 percentage points; the improvement for  $\chi_2^{\text{mass}}$  is a



**Table 2 Empirical standard deviations (mas) of the RL05 and RL06 GRACE-based equatorial effective angular momentum functions**

	$\chi_1^{\text{mass}}$	$\chi_2^{\text{mass}}$
CSR RL05	4.4 (10%)	3.2 (7%)
JPL RL05	5.3 (12%)	4.2 (9%)
GFZ RL05	7.3 (16%)	3.5 (7%)
ITSG-Grace2016	3.8 (8%)	3.1 (7%)
CSR RL06	2.2 (6%)	1.9 (4%)
JPL RL06	2.6 (7%)	2.3 (5%)
GFZ RL06	3.9 (11%)	4.0 (9%)
ITSG-Grace2018	2.2 (6%)	2.3 (5%)

The smallest empirical standard deviations of the RL05 and RL06 solutions are marked in *italics*

bit smaller (about 3 percentage points). ITSG-Grace2016 shows the smallest empirical standard deviation among the RL05 solutions, while CSR shows the smallest empirical standard deviation among the RL06 solutions.

The GRACE-based effective angular momentum functions are compared with the reduced geodetic excitations (mass-related part)  $\chi^{\text{C04-NE}}$  and  $\chi^{\text{C04-ESMGFZ}}$ . Table 3 shows the root mean square (RMS) differences and correlation coefficients between the excitation functions derived from GRACE data (CSR RL05, CSR RL06, JPL RL05, JPL RL06, GFZ RL05, GFZ RL06, ITSG-Grace2016, ITSG-Grace2018) and the excitation functions based on space-geodetic observations. It can be seen that the agreement could be significantly improved by the release update, especially in the case of JPL. The best agreement can be seen between the excitation functions from ITSG-Grace2018 and C04-NE.

**Polar motion excitation: individual effects from subsystems**

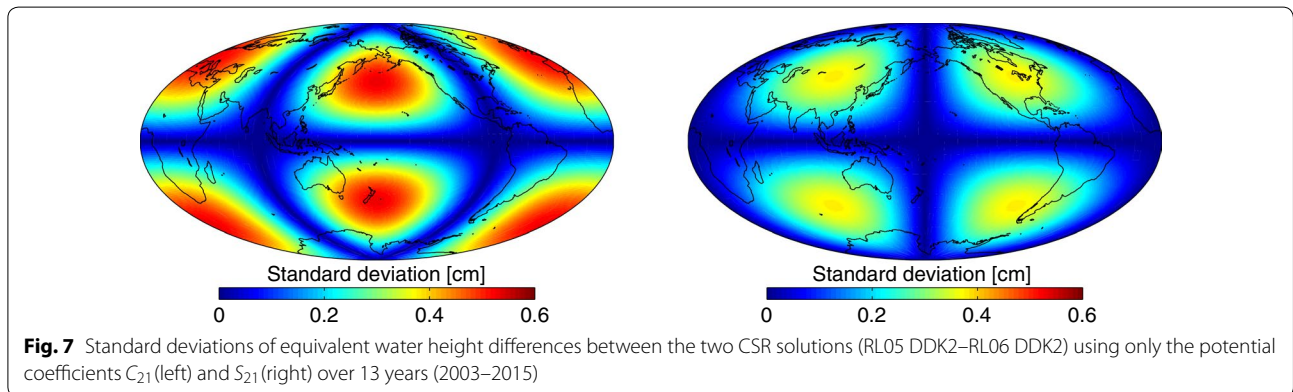
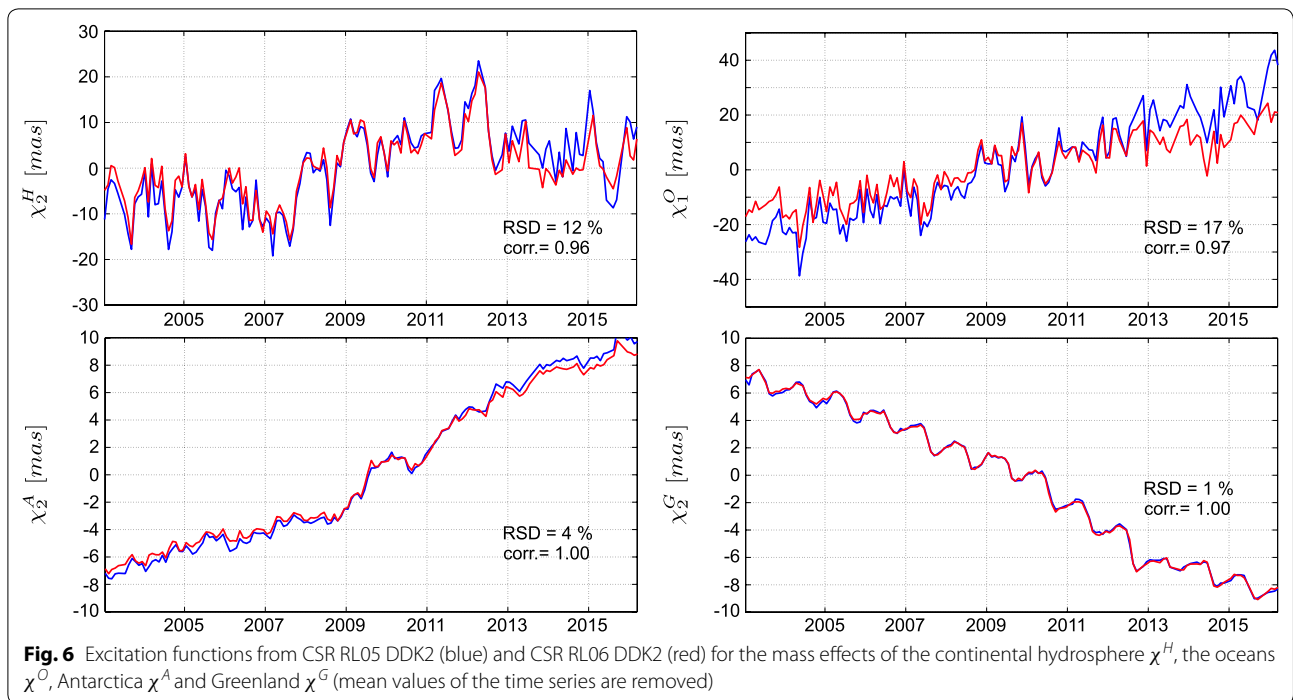
This section presents an analysis of the contributions of individual Earth subsystems to the mass-related excitation of polar motion. Therefore, the integral GRACE

**Table 3 RMS differences (mas)/correlation coefficients between the GRACE-based equatorial effective angular momentum functions and the mass-related part of the geodetic excitation of polar motion**

	$\chi_1^{\text{mass}}$		$\chi_2^{\text{mass}}$	
	C04-NE	C04-ESMGFZ	C04-NE	C04-ESMGFZ
CSR RL05	7.1/0.76	8.4/0.76	9.9/0.97	9.3/0.96
JPL RL05	9.6/0.57	13.0/0.35	11.4/0.93	11.6/0.90
GFZ RL05	7.3/0.75	8.7/0.74	10.6/0.95	10.1/0.94
ITSG-Grace2016	6.7/0.79	8.9/0.71	11.1/0.95	10.9/0.93
CSR RL06	6.2/0.82	7.3/0.84	9.3/0.97	8.9/0.96
JPL RL06	6.9/0.78	8.0/0.78	10.1/0.97	9.7/0.95
GFZ RL06	7.8/0.71	8.2/0.77	11.2/0.95	11.3/0.92
ITSG-Grace2018	6.2/0.84	7.0/0.87	9.3/0.98	8.7/0.97

The smallest RMS differences and largest correlation coefficients of all GRACE solutions are marked in *italics*

signal needs to be separated using filter techniques and masks. As shown before, the signal-to-noise ratio of the GRACE results could be significantly improved by the release update from RL05 to RL06. Thus, it can be expected that also the quantification of individual mass-related contributions to polar motion excitation on the basis of GRACE observations benefits strongly from the improvement. Figure 6 shows the resulting excitation functions from CSR RL05 DDK2 and CSR RL06 DDK2 for the mass effects of the continental hydrosphere  $\chi^H$ , the oceans  $\chi^O$ , and the cryosphere. The latter are presented separately for Antarctica  $\chi^A$  and Greenland  $\chi^G$ . Larger discrepancies between the old and new releases are visible for  $\chi^H$  (RSD = 12%) and  $\chi^O$  (RSD = 17%). This can be explained by the fact that the change of the  $C_{21}$  series in the course of the release update has a dominant effect on the oceanic mass estimates, and changes in  $S_{21}$  dominate the mass estimates in the continental regions of North America,



South America and Asia as well as in the Indian Ocean (see Fig. 7). In contrast, the changes for  $\chi^A$  (RSD = 4%) and  $\chi^G$  (RSD = 1%) are relatively small as the mass estimates for Antarctica and Greenland are only slightly influenced by the change of the potential coefficients  $C_{21}$  and  $S_{21}$  from RL05 to RL06. Figure 8 shows the differences of the excitation functions from the CSR, JPL, GFZ and ITSG GRACE gravity models with respect to the mean of all four excitation functions. The corresponding empirical standard deviations are given in Table 4. The release update improved the agreement between the four GRACE solutions by about 7 percentage points for  $\chi_1^O$ , 4 percentage points for  $\chi_2^H$ , 1 percentage point for  $\chi_2^A$ , and only 0.2 percentage points

for  $\chi_2^G$ . Note that for the oceans  $\chi_1$  is the prominent component, whereas  $\chi_2$  is dominant for continental hydrology, Antarctica and Greenland. Again, ITSG-Grace2016 exhibits the smallest empirical standard deviation among the RL05 solutions, while CSR features the smallest empirical standard deviation among the RL06 solutions.

In Fig. 9 and Table 5, we present a comparison of the GRACE-derived individual polar motion excitation functions with independent data exemplarily for the oceans (model results for the contributions of the continental hydrosphere and the two continental ice sheets are characterized by higher uncertainties). The polar motion excitation functions for the oceanic mass effect from

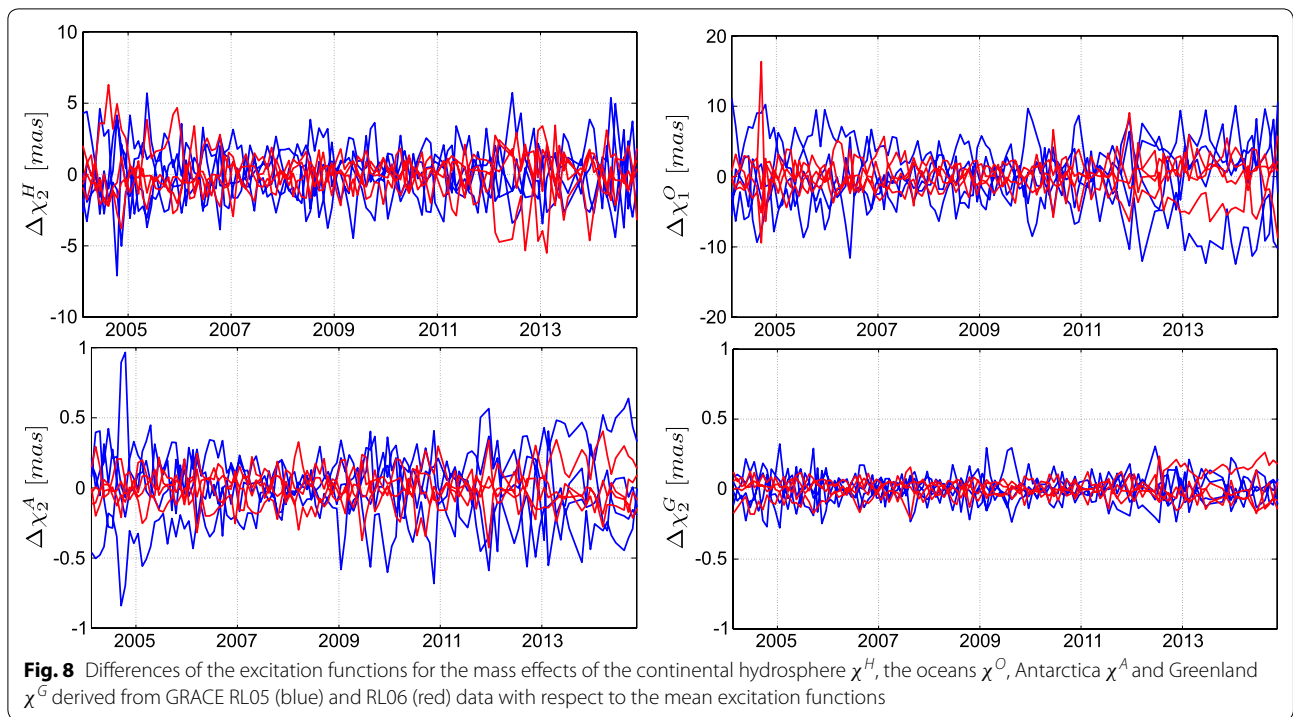


**Fig. 8** Differences of the excitation functions for the mass effects of the continental hydrosphere  $\chi^H$ , the oceans  $\chi^O$ , Antarctica  $\chi^A$  and Greenland  $\chi^G$  derived from GRACE RL05 (blue) and RL06 (red) data with respect to the mean excitation functions

**Table 4 Empirical standard deviations (mas) of the GRACE-based equatorial effective angular momentum functions for the continental hydrosphere (H), oceans (O), Antarctica (A) and Greenland (G)**

	$\chi_2^H$	$\chi_1^O$	$\chi_2^A$	$\chi_2^G$
CSR RL05	1.6 (9%)	3.5 (13%)	0.3 (3%)	0.1 (1%)
JPL RL05	1.9 (10%)	4.2 (15%)	0.2 (3%)	0.1 (1%)
GFZ RL05	2.0 (11%)	5.9 (21%)	0.3 (3%)	0.1 (1%)
ITSG-Grace2016	<i>1.6 (9%)</i>	<i>2.8 (10%)</i>	<i>0.2 (2%)</i>	<i>0.1 (1%)</i>
CSR RL06	<i>1.0 (5%)</i>	<i>1.8 (7%)</i>	<i>0.1 (2%)</i>	<i>0.1 (1%)</i>
JPL RL06	1.2 (6%)	2.1 (8%)	0.1 (1%)	0.1 (1%)
GFZ RL06	2.2 (12%)	3.2 (12%)	0.2 (2%)	0.1 (1%)
ITSG-Grace2018	1.0 (6%)	1.9 (7%)	0.1 (1%)	0.1 (1%)

The smallest empirical standard deviations of the RL05 and RL06 solutions are marked in italics

GRACE data and from ocean models differ significantly with respect to their trends. However, the trends of the ocean models cannot be viewed as realistic as they are Boussinesq models that conserve volume rather than mass. Mass conservation is reached by adding a homogeneous shell of mass at every time step. Therefore, the trends of all series are reduced before the computation of RMS differences and correlation coefficients (Table 5). The update from RL05 to RL06 improved the agreement of the GRACE-derived oceanic effective angular momentum functions with modeled mass-related oceanic polar motion excitation functions by about 5 percentage points for CSR, 15 percentage points for JPL, 4 percentage points for GFZ and 5 percentage points for ITSG. In general, the agreement of the GRACE-derived oceanic effective angular momentum functions with ocean

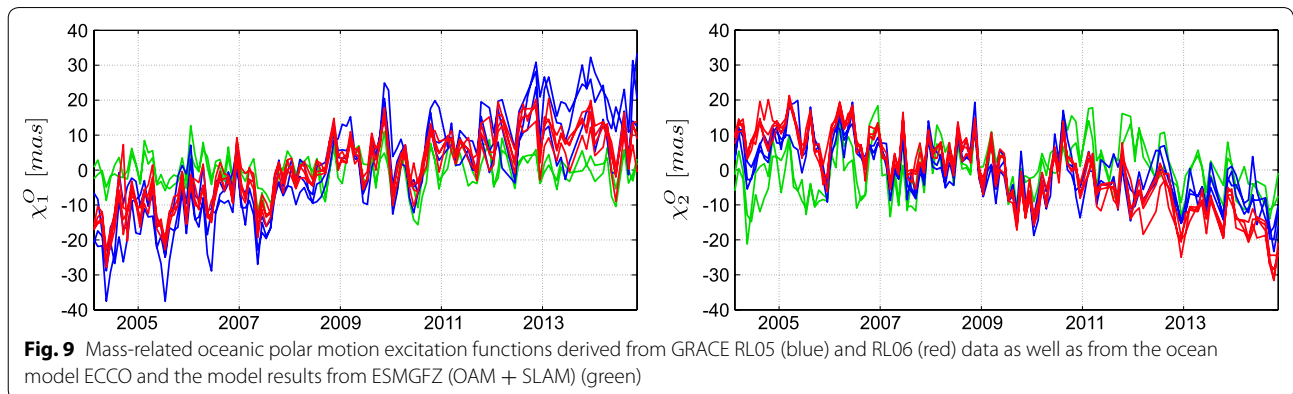


**Fig. 9** Mass-related oceanic polar motion excitation functions derived from GRACE RL05 (blue) and RL06 (red) data as well as from the ocean model ECCO and the model results from ESMGFZ (OAM + SLAM) (green)



**Table 5 RMS differences (mas)/correlation coefficients between the GRACE-based equatorial effective angular momentum functions for the oceanic mass effect and ocean model results**

	$x_1^O$		$x_2^O$	
	ECCO (OAM)	ESMGFZ (OAM+SLAM)	ECCO (OAM)	ESMGFZ (OAM+SLAM)
CSR RL05	5.5/0.49	4.4/0.72	6.0/0.61	6.0/0.66
JPL RL05	8.3/0.35	6.8/0.64	7.7/0.41	6.8/0.60
GFZ RL05	5.7/0.51	4.9/0.69	6.8/0.50	6.7/0.58
ITSG-Grace2016	5.3/0.58	4.0/0.79	6.5/0.54	6.1/0.65
CSR RL06	4.6/0.60	3.9/0.76	5.7/0.66	5.2/0.75
JPL RL06	5.0/0.57	4.4/0.71	5.9/0.63	5.4/0.74
GFZ RL06	5.3/0.58	4.8/0.69	6.2/0.58	5.2/0.76
ITSG-Grace2018	4.5/0.62	3.9/0.76	5.5/0.68	5.0/0.78

Trends have been removed prior to the determination of the RMS differences and correlation coefficients

The smallest RMS differences and largest correlation coefficients of all GRACE solutions are marked in italics

model results from ESGMFZ is better than with ocean model results from ECCO. The best agreement can be seen between the oceanic effective angular momentum functions from ITSG-Grace2018 and ESGMFZ (OAM + SLAM).

## Conclusion

With the GRACE Release 06 solution, the estimation of mass redistributions has significantly been improved, and the noise in the GRACE gravity field solutions has been reduced. Furthermore, the consistency of the analyzed GRACE solutions of CSR, JPL, GFZ and ITSG was increased. Concerning polar motion excitation, in particular the change in the potential coefficients  $C_{21}$  and  $S_{21}$  (about 32% RL05/RL06) due to the change of the mean pole model from cubic to linear plays a great role. On the other hand, the update of the AOD1B product has only a minor influence. The changes in the potential coefficients  $C_{21}$  and  $S_{21}$  amount to only 14 and 8% respectively. While the integral effect of the mass-related polar motion excitation can be directly derived from the potential coefficients  $C_{21}$  and  $S_{21}$  (GSM + GAC), the determination of individual contributions from the Earth's subsystems is based on the full set of potential coefficients (GSM + GAD) and requires adequate filtering and masking. Due to the improvement of the signal-to-noise ratio in the RL06 gravity field models, the decorrelation filter DDK3 delivers good results (this is not the case for the RL05 gravity field models). Looking at the GRACE-based results for the integral mass-related polar motion excitation, the change due to the update from RL05 to RL06 is about 15%. The changes of the time series of  $C_{21}$  and  $S_{21}$  have a large impact on the oceanic (17%) and hydrological excitation (12%), but the effect on the contributions from ice loss in Antarctica (4%) and Greenland (1%) is

small. The trend, in particular of the oceanic mass variation, is significantly reduced in RL06, and the agreement of the excitation functions computed from the CSR, JPL, GFZ and ITSG solutions was improved. For the integral polar motion excitation, the empirical standard deviations of the four solutions amount to 3.8 to 7.3 mas for RL05 and only to 2.2 to 3.9 mas for RL06. The largest improvement can be seen for the mass-related polar motion excitation of the ocean (7 percentage points), followed by the continental hydrology (4 percentage points), Antarctica (1 percentage point) and Greenland (0.2 percentage points). A validation with external results is difficult due to the relatively large uncertainties of geophysical models. For the ocean, our results showed that the latest release update led to a generally higher agreement between the excitation functions from GRACE and model data (improvement 4 to 15 percentage points), where the excitation functions from the ITSG-Grace2018 solution and from the ESGMFZ model agree best. The agreement of the GRACE-derived effective angular momentum functions with the mass-related part of the geodetic excitation could be improved by 2 to 7 percentage points due to the release update. The time series of polar motion excitation derived from ITSG-Grace2018 and C04-NE shows the highest agreement.

## Authors' contributions

FG planned the research, conducted the data processing and analysis and wrote the majority of the paper. FS contributed significantly to the writing of the manuscript. All authors read and approved the final manuscript.

## Acknowledgements

The GRACE satellite mission was operated and maintained by NASA (National Aeronautics and Space Administration) and DLR (Deutsches Zentrum für Luft- und Raumfahrt). The GRACE gravity field solutions were provided by the GRACE science teams of CSR, JPL and GFZ as well as by the ITSG of the Graz University of Technology. We are grateful to the IERS for providing polar motion observation series and geophysical fluids data. Open access was

supported by the TUM Open Access Publishing Funds. We also thank the two reviewers for their suggestions and comments, which greatly improved the manuscript.

#### Competing interests

The authors declare that they have no competing interests.

#### Availability of data and materials

All GRACE-derived polar motion excitation functions from DGF-TUM can be provided on request.

#### Funding

These studies are performed in the framework of the project CIEROT (Combination of geodetic space observations for estimating cryospheric mass changes and their impact on Earth rotation) funded by the German Research Foundation (DFG) under Grant No. GO 2707/1-1.

#### Publisher's Note

Springer Nature remains neutral with regard to jurisdictional claims in published maps and institutional affiliations.

Received: 13 August 2018 Accepted: 3 December 2018

Published online: 12 December 2018

#### References

- Adhikari S, Ivins ER (2016) Climate-driven polar motion: 2003–2015. *Sci Adv* 2:1501693
- Barnes RTH, Hide R, White AA, Wilson CA (1983) Atmospheric angular momentum fluctuations, length-of-day changes and polar motion. *Proc R Soc Lond Ser A* 387:31–73
- Bettadpur S (2012) UTCSR level-2 processing standards document for level-2 product release 0005. Technical Report GRACE, 327–742
- Bettadpur S (2018) UTCSR level-2 processing standards document for level-2 product release 0006. Technical Report GRACE, 327–742
- Bizouard C, Lambert S, Becker O, Richard JY (2014) Combined solution C04 for earth rotation parameters consistent with international terrestrial reference frame. [http://hpiers.obspm.fr/iers/eop/eopc04\\_05/C04.guide.pdf](http://hpiers.obspm.fr/iers/eop/eopc04_05/C04.guide.pdf). Version 5, June 2009
- Brzeziński A (1992) Polar motion excitation by variations of the effective angular momentum function: considerations concerning deconvolution problem. *Manuscr Geod* 17(1):3–20
- Chen W, Li J, Ray J, Cheng M (2017) Improved geophysical excitations constrained by polar motion observations and GRACE/SLR time-dependent gravity. *Geod Geodyn* 8:377–388
- Chen JL, Wilson CR, Ries JC, Tapley BD (2013) Rapid ice melting drives Earth's pole to the east. *Geophys Res Lett* 40:2625–2630
- Cheng M, Tapley BD, Ries JC (2013) Deceleration in the Earth's oblateness. *J Geophys Res* 118:1–8
- Dahle C, Flechtner F, Gruber C, König D, König R, Michalak G, Neumayer K-H (2012) GFZ GRACE level-2 processing standards document for level-2 product release 0005. Scientific technical report STR12/02-data, revised edition, 2013 January
- Dahle C, Flechtner F, Murböck M, Michalak G, Neumayer H, Abrykosov O, Reinhold A, König R (2018) GFZ level-2 processing standards document for level-2 product release 06. Scientific technical report STR-data; 18/04, revised edition, 2018 August
- Dobslaw H, Dill R (2018) Predicting Earth orientation changes from global forecasts of atmosphere-hydrosphere dynamics. *Adv Space Res* 61(4):1047–1054
- Dobslaw H, Flechtner F, Bergmann-Wolf I, Dahle C, Dill R, Esselborn S, Sasgen I, Thomas M (2013) Simulating high-frequency atmosphere-ocean mass variability for de-aliasing of satellite gravity observations: AOD1B RL05. *J Geophys Res* 118(7):3704–3711
- Dobslaw H, Wolf I, Dill R, Poropat L, Thomas M, Dahle C, Esselborn S, König R, Flechtner F (2017a) A new high-resolution model of non-tidal atmosphere and ocean mass variability for de-aliasing of satellite gravity observations: AOD1B RL06. *Geophys J Int* 211(1):263–269
- Dobslaw H, Bergmann-Wolf I, Dill R, Poropat L, Flechtner F (2017b) Product description document for AOD1B release 06. Technical report GRACE, 327–750
- Fagiolini E, Flechtner F, Horwath M, Dobslaw H (2015) Correction of inconsistencies in ECMWF's operational analysis data during de-aliasing of GRACE gravity models. *Geophys J Int* 202(3):2150–2158
- Flechtner F, Dobslaw H, Fagiolini E (2015) AOD1B product description document for product release 05. Technical report GRACE, 327–750
- Gross R (1992) Correspondence between theory and observations of polar motion. *Geophys J Int* 109:162–170
- Gross R (2007) Earth rotation variations-long period. In: Schubert G (ed) *Treaties on geophysics*. Elsevier, New York, pp 239–294
- Göttl F, Schmidt M, Seitz F, Bloßfeld M (2015) Separation of atmospheric, oceanic and hydrological polar motion excitation mechanisms based on a combination of geometric and gravimetric space observations. *J Geod* 89:377–390
- Göttl F (2013) Kombination geodätischer Raumberechnungen zur Bestimmung von geophysikalischen Anregungsmechanismen der Polbewegung. In: *Deutsche Geodätische Kommission vol. C741*. Verlag der Bayerischen Akademie der Wissenschaften, Germany
- Ivins ER, James TS, Wahr J, Schrama O, Ernst J, Landerer FW, Simon KM (2013) Antarctic contribution to sea level rise observed by GRACE with improved GIA correction. *J Geophys Res Solid Earth* 118:3126–3141
- Jungclauss JH, Fischer N, Haak H, Lohmann K, Marotzke J, Matei D, Mikolajewicz U, Notz D, von Storch JS (2013) Characteristics of the ocean simulations in the Max Planck Institute Ocean Model (MPIOM) the ocean component of the MPI-Earth system model. *J Adv Model Earth Syst* 5(2):422–446
- Kusche J (2007) Approximate decorrelation and non-isotropic smoothing of time-variable GRACE-type gravity field models. *J Geod* 81:733–749
- Malgorzata W, Nastula J, Salstein D (2017) Hydrological excitation of polar motion by different variables from the GLDAS models. *J Geod* 91:1461–1473
- Mayer-Gürr T, Behzadpour S, Ellmer M, Kvas A, Klinger B, Zehentner N (2016) ITSG-Grace2018-monthly and daily gravity field solutions from GRACE. <https://doi.org/10.5880/icgem.2016.007>
- Mayer-Gürr T, Behzadpour S, Ellmer M, Kvas A, Klinger B, Strasser S, Zehentner N (2018) ITSG-Grace2018-monthly, daily and static gravity field solutions from GRACE. <https://doi.org/10.5880/ICGEM.2018.003>
- Meyrath T, van Dam T (2016) A comparison of interannual hydrological polar motion excitation from GRACE and geodetic observations. *J Geod* 99:1–9
- Petit G, Luzum B, IERS Conventions (2010) Technical report IERS technical note no. 36, Verlag des Bundesamts für Kartographie und Geodäsie, Frankfurt am Main, Germany
- Swenson S, Chambers D, Wahr J (2008) Estimating geocenter variations from a combination of GRACE and ocean model output. *J Geophys Res* 113:808410
- Wahr J, Molenaar M, Bryan F (1998) Time variability of the Earth's gravity field: hydrological and oceanic effects and their possible detection using GRACE. *J Geophys Res* 103:30205–30229
- Wahr J (2005) Polar motion models: angular momentum approach. In: Plag HP, Chao B, Gross R, van Dam T (eds) *Proceedings of the workshop: forcing of polar motion in the Chandler frequency band—a contribution to understanding international climate changes*. Cahiers du Centre Europeen de Geodynamique et de Seismologie, Luxembourg, pp 89–102
- Watkins MM, Yuan D (2014) JPL level-2 processing standards document for level-2 product release 05.1. Technical report GRACE, 327–744
- Yuan D (2018) JPL level-2 processing standards document for level-2 product release 06. Technical report GRACE, 327–744
- Zhou YH, Salstein DA, Chen JL (2006) Revised atmospheric excitation function series related to Earth variable rotation under consideration of surface topography. *J Geophys Res* 111:12108